Lithium-ion rechargeable batteries

Sid Megahed
Rayovac Corporation, Madison, WI 53744-4960 (USA)

Bruno Scrosati
Dipartimento di Chimica, Università 'La Sapienza', 00185 Rome (Italy)

(Received June 16, 1994; accepted in revised form June 27, 1994)

Abstract

The large availability of insertion electrodes capable to exchange substantial quantities of lithium ions with relatively fast kinetics, has promoted the development of various types of rechargeable lithium batteries having different design, size, capacity, power and energy capabilities. All these lithium batteries offer a series of considerable specific advantages, such as high energy density and relatively low cost. However, their widespread utilization is still influenced by the high reactivity of the metal which, from one side assures the high energetic content, from the other induces safety hazards and limited cycleability. Attempts to overcome this shortcoming have resulted in the development of batteries where the lithium metal is most commonly replaced by a carbon electrode. Penalties in energy density in respect to the lithium systems are counterbalanced by an expected safer and longer cycle life from the carbon systems. Although a very recent innovation, the rocking-chair idea has already found enthusiastic support in many research laboratories which are presently involved in its investigation and development. As a result of this, small size, lithium rocking-chair batteries or, as otherwise named 'lithium-ion batteries', are currently under development in Japan, USA and Europe. In this review paper we describe the properties of the anode, cathode and electrolyte materials which presently seem to be the most promising for the development of these batteries, and we will attempt to evaluate the impact that the rocking-chair concept may ultimately have on the progress of rechargeable lithium battery technology. We will also summarize the status of practical rocking-chair batteries for various emerging applications.

1. Introduction

The rapid development of innovative technologies poses particular urgency to the need for new and efficient power source systems. This need is motivated by a series of crucial demands which range from the request of an efficient utilization of our energy resources to the constraints imposed by environmental protections. This has favored the search for advanced, high energy, electrochemical systems which would be capable of replacing the conventional batteries for a more efficient and less-polluting environment. For instance, high energy density, rechargeable batteries are needed today to replace bulky lead/acid batteries for the development of long range electric vehicles, with consequent decrease in oil consumption and, most importantly, with improvements in the air quality of large urban areas. Furthermore, reliable batteries are in demand for off-peak electric energy storage, as emergency power supplies in remote rural areas and as storage systems for intermittent energy sources, such as

0378-7753/94/$07.00
SSDI 0378-7753(94)01956-V

solar and wind. Finally, advanced and environmental friendly batteries would be highly desirable in the electronic consumer market to replace the nickel–cadmium batteries or, even, the most common zinc–carbon dry cells, with the final goal of limiting the risk associated with their waste disposal.

For an effective development of a high energy density battery, the use of high capacity electrode materials is the essential factor. Alkali metals are the obvious choices and, indeed, the most promising types of advanced batteries currently under production are based on these metals as negative electrodes. For example, the advanced system which appears to be closest to industrial production, namely the sodium–metal chloride (e.g. $NiCl_2$) battery uses a molten sodium anode. A lithium–aluminum alloy is the anode of another system, of present interest for advanced electrochemical storage, i.e., the lithium–iron disulfide battery. Both these batteries are today regarded as serious candidates for the large-scale development of efficient electric vehicles; however, they operate at temperatures much higher than ambient, namely at about 350 and 450 °C, respectively. Such high operational temperatures introduce some serious technological problems. First, the requirement of expensive materials to resist the highly corrosive molten electrode (e.g., Na and S) and electrolyte (e.g., LiCl–BiBr–KBr) components, and secondly, the addition to the electrochemical system itself of a thermal control unit in order to keep the battery running. The latter does not appear to be a crucial problem for the off-peak (load-leveling) or, even for the electric vehicle applications. However, they are unacceptable for a more versatile use where operation may be typically expected at 'ambient' temperature, ranging from -10 to 40 °C depending on the geographic location. Therefore, the development of ambient temperature, high-energy batteries is a major task today, and accordingly many laboratories throughout the world are carrying out research aiming to reach this important goal.

The most promising results in the research of new alternative power sources have been so far with electrochemical systems using a lithium anode, a lithium-ion conducting electrolyte and a lithium-ion-accepting cathode material. The choice of the anode material is restricted by the already stressed need for a high energy content which is unavoidably linked to the use of an alkali metal as the main anodic material. Lithium is generally preferred since it is more easily handled than other alkali metals, and most significantly, the lightest and the most electronegative of the family. In fact, lithium metal has an extremely high value of specific capacity, namely, 3.86 Ah g^{-1}.

The choice of the cathode is somewhat more flexible since various materials can, in principle, assure the electrochemical balance for the overall lithium battery design. Quite reasonably, the less the extent of bonding and structure modifications of the selected cathode material, the higher the chances of the successful development of rechargeable, long-cycleable battery systems. The most suitable materials in this respect are the so-called 'insertion compounds', namely A_zB_y compounds having an open structure capable of accepting and releasing x number of lithium ions per A_zB_y mole. Accordingly, a lithium anode/intercalation cathode combination gives cells operating on a reversible electrochemical reaction, usually called a 'lithium insertion' or 'lithium intercalation' process, which may be basically described as the insertion-extraction of both mobile lithium ions and compensating electrons into a rigid host structure. The guest Li^+ ions induce reversible modifications in the host structure, while the guest electrons induce reversible changes of the oxidation state of A and thus, changes of the electronic properties of the host A_zB_y compound [1, 2].

The overall discharge process involves the dissolution of x lithium ions at the anode, their migration across the electrolyte and their insertion within the crystal structure of the host compound, while the compensating electrons travel in the external

circuit to finally be injected in the electronic band-structure of the same hosting compound. The overall charge process is just the opposite:

$$x\mathrm{Li} + \mathrm{A_zB_y} \underset{\text{discharge}}{\overset{\text{charge}}{\rightleftharpoons}} \mathrm{Li_xA_zB_y} \quad (1)$$

Therefore, any liquid or solid conducting material characterized by fast lithium ion transport can be used as an electrolyte medium for these batteries.

Common examples of liquid electrolytes are solution of lithium salts in aprotic organic solvent mixtures [3]. Crystalline or glassy compounds having vacancy or interstitial defects energetically favorable for Li^+ transport may act as solid electrolytes [4]. Finally, an important class of electrolytes suitable for lithium batteries which have a compromised solid-to-liquid structure, are polymeric membranes formed by the solvation of lithium salts in high molecular weight polymers, such as poly(ethylene oxide), PEO [5], or by liquid solutions (e.g., solutions of lithium salts in aprotic solvents) trapped in a polymer matrix (e.g., a polyacrylonitrile, PAN, matrix) [6].

The insertion electrodes most commonly used as cathodes in lithium batteries are inorganic compounds, such as transition metal dichalcogenides and oxides, characterized by layered or tunneled structures capable of providing channels for the easy access and fast mobility of the guest lithium ions. In principle, these compounds are capable of very long battery cycle life. In practice, however, the life of the battery may be limited by the cycleability of the lithium metal negative electrode. In fact, corrosion reactions may induce the growth of passivation layers on the electrode surface which greatly affect the uniformity of the plated lithium during the charge process, to an extent which may ultimately lead to a total cell failure (due to dendritic short-circuiting) or even to serious safety hazard (due to accidental short-circuiting, forced overdischarge and so forth, which induce local overheating and pressure build-up). Indeed, a few incidents have occurred, with occasional fires in equipment powered by lithium batteries, even for prototypes assembled in industrial laboratories having recognized experience in lithium battery technology. Therefore, safety is a key issue in lithium battery development at the present.

One way which has been proposed for meeting the safety requirement is to replace the lithium anode by another insertion compound, say, B_nC_m, capable of accepting and exchanging large quantities of lithium ions. In this way, rather than lithium plating and stripping as in the conventional systems, the electrochemical process at the negative side would be the uptake of lithium ions during charge and their release during discharge. Therefore, the negative B_nC_m electrode acts as a 'lithium sink' and a selected positive LiA_zB_y electrode acts as a 'lithium source' and the total electrochemical process of the B_nC_m/LiA_zB_y cell involves the cyclic transfer of x equivalents of lithium ions between the two insertion electrodes:

$$\mathrm{B_nC_m} + \mathrm{LiA_zB_y} \underset{\text{discharge}}{\overset{\text{charge}}{\rightleftharpoons}} \mathrm{Li_xB_nC_m} + \mathrm{Li_{(1-x)}A_zB_y} \quad (2)$$

These unconventional electrochemical systems may be described as concentration cells where lithium ions 'rock' from one electrodic side to the other; accordingly, these cells have been originally termed rocking-chair batteries [7] or, more recently with a series of alternative names, such as lithium-ion [8] or shuttlecock [9] batteries by Japanese industries and swing [10] batteries by European industries.

Considering the general design which involves a positive lithium-source electrode combined with a negative lithium-accepting electrode and the related nature of the electrochemical driving process, a successful operation for a RCB and its effective

competition with a metal lithium system requires some crucial conditions which should be fulfilled by the selected insertion electrodes. They are in essence:

(i) the lithium activity in the negative electrode $Li_xB_nC_m$ must be close to 1 in order to assure open-circuit voltages approaching those obtainable with the pure lithium;

(ii) the equivalent weight of both electrodes must be low in order to assure specific capacity values of practical interest;

(iii) the mobility of Li^+ ions and of electrons in both the lithium-source $Li_{(1-x)}A_zB_y$ positive electrode and in the lithium sink $Li_xB_nC_m$ negative electrode must be high in order to assure fast kinetics of the electrochemical process and thus, fast charge and discharge rates;

(iv) the voltage changes upon lithium ion uptake and release must be small in both electrodes in order to limit fluctuations during charge and discharge cycles, and

(v) both the ion-source and the ion-sink electrode must be easy to fabricate and based on non-toxic compounds, to assure low cost and environmental control.

To satisfactorily meet these conditions, insertion compounds with properties consistently different from those normally used for the 'conventional' lithium batteries, must be selected. For instance, conditions (i) and (ii) can be achieved only by using innovative materials which could assure lithium insertion voltages approaching zero (versus Li). The most popular in this respect today are carbon-type insertion compounds.

Furthermore, the achievement of the above-mentioned crucial conditions requires not only the selection of a low voltage negative but also that of a high voltage positive electrode. To date, the most popular cathodes are those having lithium insertion voltages around 4 V, namely layered lithium metal oxides of the $LiMnO_2$ type, where M = Co or Ni, and the three-dimensional, spinel-type, lithium manganese oxides.

Also, the choice of the electrolyte is crucial since the proper material must combine high ionic mobility (to reduce internal resistance with wide electrochemical stability to be compatible with the high voltage of the positive electrode) and with a lithium transference number approaching unity (to limit concentration polarizations).

In this review paper, we will briefly discuss the characteristics of the anode, cathode and electrolyte materials which are presently considered as the most promising for the development of practical lithium RCBs. We will also attempt to illustrate the performance of these batteries in comparison with other types of competitive rechargeable power sources.

2. Lithiated carbon anodes

Many carbonaceous materials have been developed and characterized in recent years for use as anodes in lithium RCBs. They include natural and synthetic graphites, petroleum coke, carbon fibers and mesocarbons, which differ, upon temperature and method of preparation, degree of crystallization and stacking order. These carbon electrodes can insert lithium according to the following basic scheme:

$$xLi + 6C \longrightarrow Li_xC_6 \tag{3}$$

where $0 < x < 1$ depending upon the type of carbon used.

The LiC_6 structure, which can also be prepared chemically under adequate temperature and pressure conditions [11], has a golden color and belongs to graphite intercalation compounds (GICs) of stage-1, where the stage number corresponds to the number of graphite layers which separate two successive intercalated planes.

The fabrication of practical carbon electrodes requires the addition of a binder, the most used being ethylene/propylene/diene monomer (EPDM) [12]. However, also

poly(vinylidene fluoride) (PVDF) [13] and poly(vinyl chloride) (PVC) [14] have been successfully used. The final shape of the electrode is generally obtained by forming a slurry of carbon, the binder and a suitable solvent. The electrode is then shaped in the desired form by a casting or pressing procedure.

Figure 1 illustrates a typical voltage–capacity curve and a derivative plot for a graphite electrode, determined by monitoring its voltage versus a lithium counter electrode during the first intercalation-deintercalation cycle. The charge promotes the intercalation of Li^+ ions within the layered structure of the graphite electrode whose voltage decreases accordingly along various distinguishable plateaus (which correspond to progressive formation of various stages of intercalated graphite), to finally reach a value approaching 0.01 V versus Li. The charge consumed in this first intercalation usually exceeds the theoretical capacity, namely 372 mAh g^{-1} for the LiC_6 composition. This increase in capacity is caused by a side process involving the decomposition of the electrolyte (refers to peak A during Li^+ intercalation in Fig. 1). The decomposition of electrolyte has been attributed to exfoliation of graphite, thus, inducing irreversible capacity. In fact, in the following discharge (lithium release) process and in all the

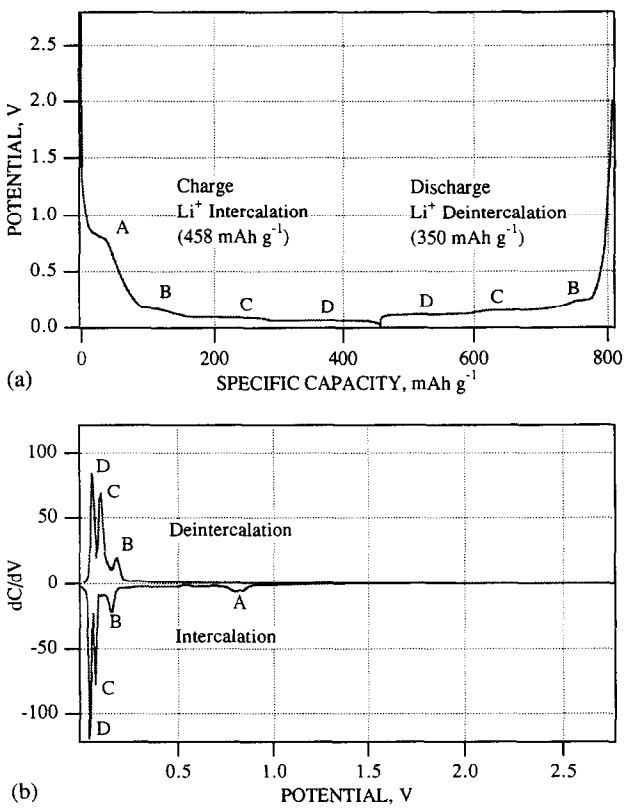

Fig. 1. (a) Voltage–capacity profile and (b) derivative plot for the first cycle intercalation-deintercalation of a synthetic graphite (KS-44) electrode using 1.0 M $LiN(CF_3SO_2)_2$/EC–DEC (50:50) electrolyte solution. The phase assignments were taken from ref. 15. A = exfoliation of graphite (irreversible); B, C, and D = lithium intercalation (reversible).

subsequent charge/discharge cycles, the capacity of the electrode approaches its expected value [15].

It is generally accepted that the first intercalation side process induces the formation on the electrode surface of a passivation layer which, being electronically insulating but ionically conducting, prevents further electrolyte decomposition while allowing ionic transfer with the solution [16]. This layer is similar to those formed on alkali metals immersed in non-aqueous solvents and commonly known as solid electrolyte interface (SEI) as described by Peled [17]. The formation of the passivation layer seems to be an essential effect in assuring the stability and the cycleability of the Li_xC_6 electrode since it provides the conditions for the desired electrochemical operation even at voltage levels which fall well below the reduction limit of the stability window of the most common electrolytes.

Indeed, the response of the carbon electrode greatly depends on the type and the composition of the electrolyte solution, especially with respect to the amount of cycleable capacity. This is clearly shown in Fig. 2, which illustrates the cycling profile of the electrode in five $LiN(CF_3SO_2)_2$ solutions [18]. The results suggest that the best response is obtained in ethylene carbonate–dimethyl carbonate (EC–DMC) solvent mixtures (see Fig. 3) and in fact, electrolytes based on these mixtures are the most commonly used for the present development of rocking-chair batteries [19, 20].

The intercalation behavior in carbon coke electrodes is somewhat different from that observed in graphite electrodes. In similarity with the latter, the former shows an initial irreversible capacity used for the formation of the passivation film; however, in contrast with graphite, the cycling profile of the coke electrodes shows no evidence of staging plateaus but rather continuous charge/discharge curves sloping between 1.2

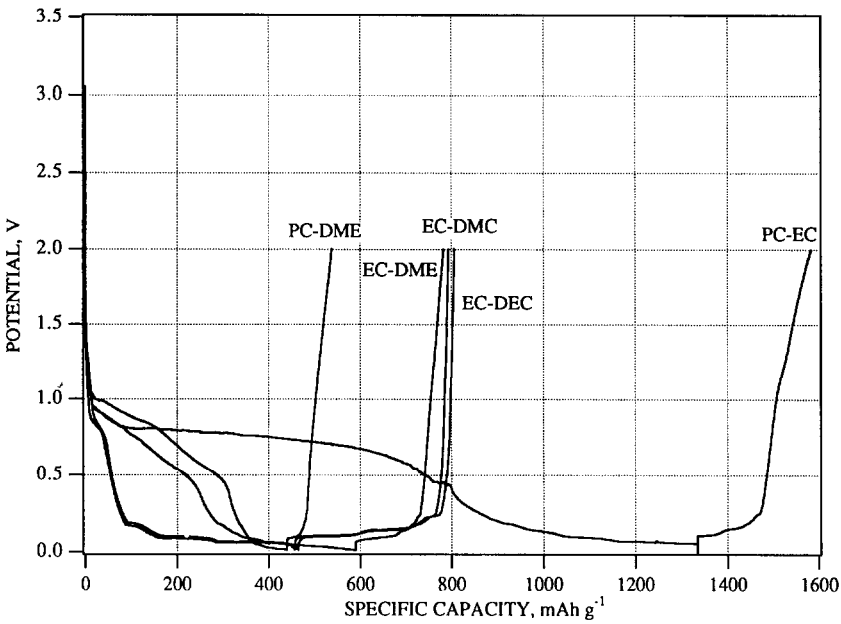

Fig. 2. Charge (Li intercalation)/discharge (Li-deintercalation) cycle of a synthetic graphite electrode in five different $LiN(CF_3SO_2)_2$ solutions (1.0 M). PC = propylene carbonate; DME = 1,2-dimethoxyethane; EC = ethylene carbonate; DMC = dimethyl carbonate, and DEC = diethyl carbonate.

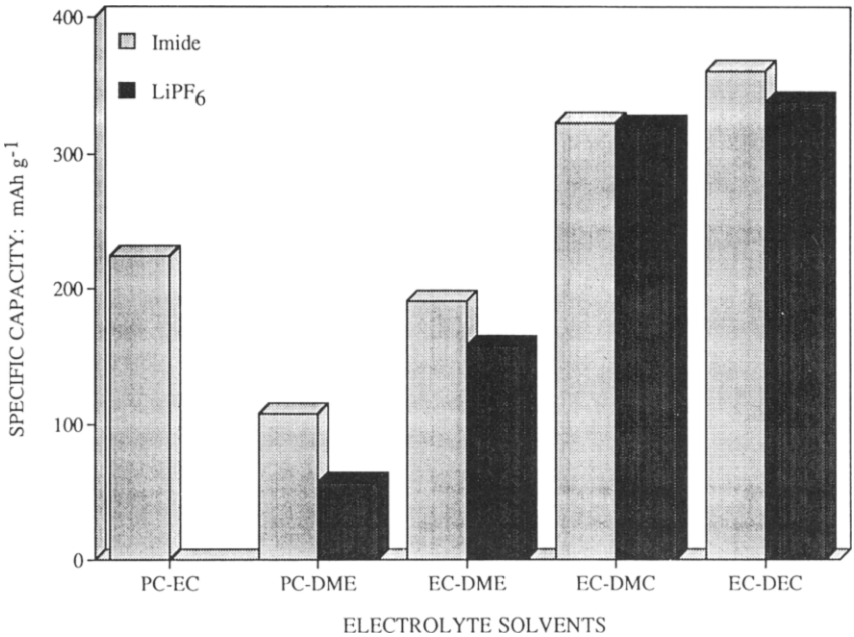

Fig. 3. Specific capacity of a synthetic graphite electrode in various lithium salt–solvent mixture solutions. PC = propylene carbonate; DME = 1,2-dimethoxyethane; EC = ethylene carbonate; DMC = dimethyl carbonate, and DEC = diethyl carbonate.

and 0.2 V [16] associated to a lithium intercalation process which cannot be extended beyond the $Li_{0.5}C_6$ composition. This depresses the capacity of the coke electrode to an average value of 186 mAh g^{-1}. In the structurally disordered coke electrodes, the intercalation process does not promote formation of staging phases, and due to its lack of crystallinity, these electrodes are not as sensitive to the nature of the electrolyte as is the case for the graphite electrodes. For instance, propylene carbonate (PC)-containing electrolytes which readily degrades graphite electrodes, can instead be used for coke electrodes. Therefore, the penalty in capacity of the latter is somewhat compensated by the gains in versatility and in rate capability which result from using the electrolytes with higher conductivity. In fact, coke electrodes are currently used in successful commercial rocking-chair batteries, such as the Sony camcorder battery.

Figure 4 illustrates a slow scan cyclic voltammetry of a carbon–coke electrode in a $LiClO_4$–PC electrolyte [14]. The trend of the curves clearly shows that the amount of cycleable charge decreases consistently passing from the first cycle to the second and third following cycles, after which a steady-state behavior is approached. Therefore, also these cyclic voltammetry results support the commonly accepted theory that in coke as well as in graphite electrodes, the initial loss of charge is followed by a stable and reproducible response. However, the voltammetric curves do not provide conclusive evidence for the proposed passivation mechanism. In fact, by closely examining the shape of the first cycle of Fig. 4, one can detect a shoulder in the cathodic (lithium uptake) scan (at about 0.7 V versus Li) and no corresponding discontinuity in the following anodic curve. This irreversible effect is likely to be associated with the above stressed passivation phenomenon. However, other effects, more directly related to the feature of the lithium insertion process, may contribute as well. In fact, considering

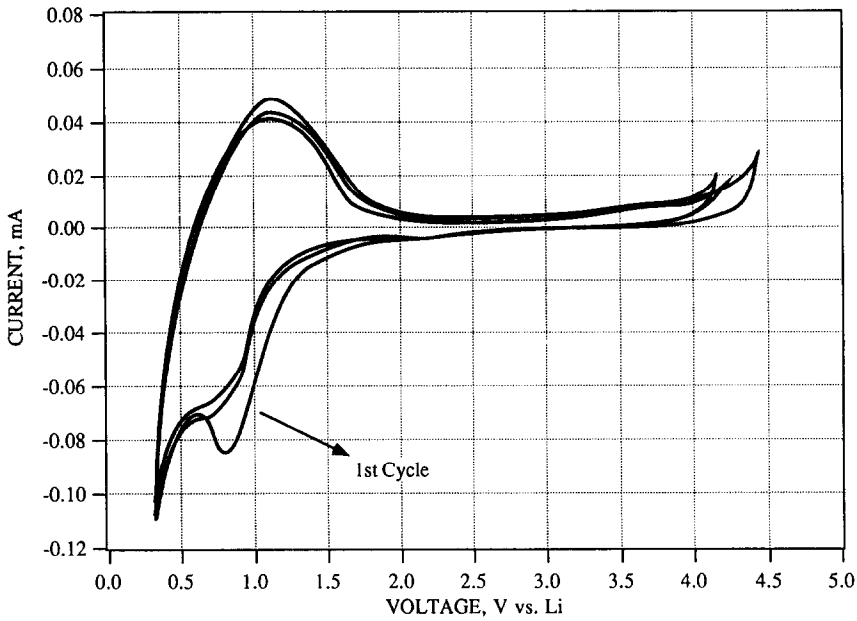

Fig. 4. Cyclic voltammetry of Li_xC_6 electrode in the $LiClO_4$–PC electrolyte at room temperature; counter electrode: Li; scan rate: 0.1 mV s^{-1}.

that the structure of the carbon electrode may be described as a combination of distorted layered graphite stacks [21], it is reasonable to assume that different sites, with different coordinating energy, are available for accommodating the initial incoming lithium ions.

Accordingly, the initial loss of charge could be in part also associated with those fractions of lithium ions which are stored in strongly screened lattice positions from where they cannot be easily removed by the electrochemical reverse process. In this connection, it is important to point out that initial irreversible uptake of guest ions is a very common phenomenon in insertion electrochemical processes, which has been established in electrodes such as Li_xNiO_y, Li_xWO_3 and which in fact has been postulated also to occur in the Li_xC_6 electrode of direct interest here [22, 23].

Attempts to obtain further information on the effective mechanism of the carbon electrode have been pursued using impedance analysis, a technique which has been successfully used to detect passivation and growth of film formation on lithium metal electrodes in contact with a variety of liquid [24] and solid [25] electrolytes. Figure 5 illustrates the response in the $-jZ''$–Z' plane of a Li_xC_6 coke electrode observed at $x=0, x=0.27$ and $x=0.52$ compositions in a cell using $LiClO_4$–PC as liquid electrolyte [14]. The response clearly reveals that the middle frequency semicircle, which is associated with the interfacial resistance, increases with increasing lithium content. However, this result is not conclusive in fully clarifying the electrode mechanism. On one hand, the expansion of the semicircle could well be attributed to an increase of the interfacial resistance due to the formation of a passivation layer, but on the other hand, the development of a second semicircle, which could clearly distinguish the effect of this layer from other interfacial phenomena, is not detected in the spectra of Fig. 5.

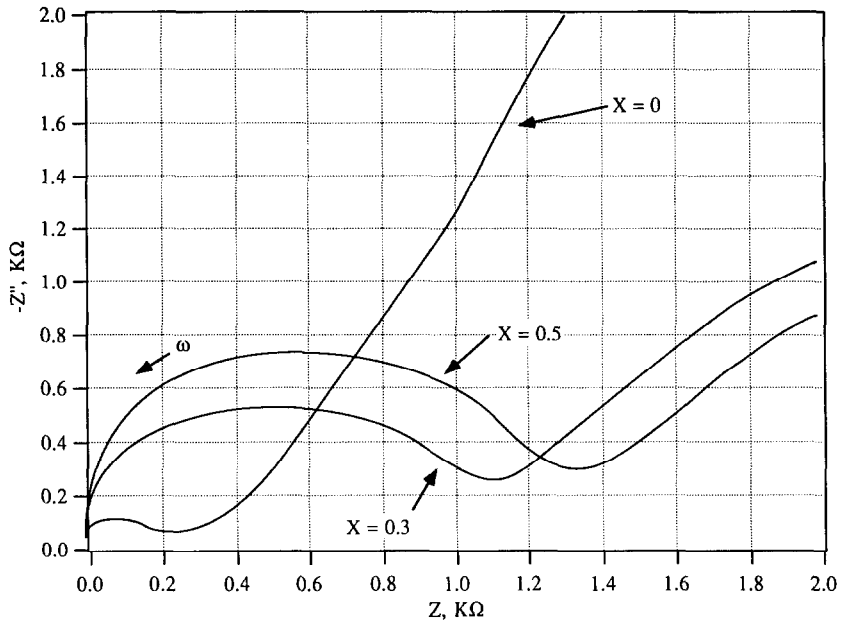

Fig. 5. Impedance response of an Li_xC_6 electrode in the $LiClO_4$–PC electrolyte at various compositions ($x=0$, $x=0.27$, and $x=0.52$); room temperature; Li: counter. From ref. 14.

More recent impedance studies carried out on a C–$LiCoO_2$ rocking-chair cell have shown that the semicircle associated with the carbon electrode expanded with increasing cycle number while that associated with the $LiCoO_2$ electrode remained almost constant [26]. This impedance result, combined with those obtained by scanning electron microscope (SEM) analyses of the carbon electrode surface after prolonged cycling, seems to suggest that it is this electrode which mostly affects the response of the overall rocking-chair cell. Therefore, the full clarification of the mechanism of the electrochemical intercalation of lithium ions is obviously a crucial requirement in view of the evaluation of the effective role that the Li_xC_6 electrode may exert in the development of reliable RCBs and further work should certainly be devoted to this important aspect.

Another point of concern in determining the use of the Li_xC_6 electrode as a replacement for the lithium metal electrode, is in the respective values of the specific capacity, since that of the former, i.e., 0.186 Ah g^{-1} for cokes ($x=0.5$) and 0.372 Ah g^{-1} for graphite ($x=1$), is more than one order of magnitude lower than that of the latter (3.86 Ah g^{-1}). Admittedly, one has to recall that, because of the poor cycleability of the metal, an excess of lithium, generally estimated four times higher than the theoretical amount, is required to assure acceptable life to conventional LiA_zB batteries. On the other hand, also under this consideration, the specific capacity of lithiated carbon remains lower than that of metal lithium and this reflects in lower attainable energy density values for carbon RCBs in comparison with metal lithium batteries. The penalty in energy density, however, is counterbalanced by the gained safety and cycleability. In addition, there are indications that by proper preparation procedures, which may involve the incorporation of foreign additives in the carbon structure [27],

electrodes with capacity exceeding the 372 mAh g^{-1} value are expected to be available in the near future [28].

Also important in the evaluation of the Li_xC_6 electrodes is the determination of the value of the diffusion coefficient of the Li^+ ions throughout the solid framework of the carbonaceous host structure. As pointed out by condition (iii), the diffusion of the Li^+ ions controls the kinetics of the electrochemical process and thus the power capability of the related battery. Surprisingly, very little attention has been dedicated to this aspect and accordingly, few diffusion data are available in the literature. Guyomard and Tarascon [12] have reported results obtained using a transient technique which suggested that the diffusion coefficient of lithium in coke electrode decreases linearly during insertion, remaining, however, confined between acceptable values, i.e., around 10^{-8} to 10^{-9} cm^2 s^{-1}. As a comparison, one may quote the value of $D_{Li^+} = 10^{-9}$ cm^2 s^{-1} in Li_xTiS_2, namely in one of the most popular intercalation electrodes [29]. Therefore, on the basis of these results, one might assume that lithiated carbon electrodes have good rate capabilities. Obviously, the rate capability of the carbon electrodes may vary according to their surface morphology. However, care has to be taken to control the surface area to be about 10 m^2 g^{-1} to assure safe operation.

Attention should also be paid to fulfill condition (iv) which recommends small voltage fluctuation upon cell cycling. This condition is difficult to obtain with coke Li_xC_6 electrodes since their voltage varies as much as 1.2 V upon the exchange of the total removable and cycleable lithium ($x = 0.5$). Generally, sloping voltage profiles in intercalation electrodes may be associated with large changes in the electrochemical potentials of both the active ionic, e.g., of the Li^+ ions, and the electronic species in the host solid medium [30]. In the case of Li_xC_6, one may then assume that the observed sloping voltage is associated with strong interactions between the Li^+ ions and the carbon host structure, and/or to large perturbation of the host's electronic configurations. Flatter charge/discharge curves are offered by structurally ordered graphite electrodes, and thus the latter are most commonly selected in the latest trend of RCB development. Possibly, some attention should be also devoted to the characterization of alternative anode materials where a lithium activity approaching one in the lithium-rich state is not the sole requirement, but also where a limited variation in the ionic and electronic electrochemical potentials upon the insertion-deinsertion process is taken into consideration. This approach is currently pursued in our laboratory with preliminary promising results [31].

3. High voltage cathodes

Most commonly, layered lithium oxides and spinel lithium manganese oxide have been selected as preferred cathode materials for the RCB development. Layered lithium metal oxides, of the general formula $LiMO_2$ (where M = Co or Ni) have a rock salt structure where lithium and transition metal cation occupy alternate layers of octahedral sites in a distorted cubic close-packed oxygen–ion lattice. The layered MO_2 framework provides a two-dimensional interstitial space which allows for easy extraction of lithium ions. More details on the structural properties of these compounds may be found in more specialized and focused review papers [32].

The important aspect is that, being capable of releasing lithium ions, $LiMO_2$ compounds behave as lithium source electrodes, and thus they can be very conveniently coupled with the carbon electrode to form a $C/LiMO_2$ battery in its fully discharged state. The activation of this battery requires a 'charging' step involving the removal of lithium ions from the $LiMO_2$ electrode and their insertion into the carbon electrode,

according to a reversible, rocking-chair (compare eqn. (2)) process of the type:

$$LiMO_2 + 6C \underset{\text{discharge}}{\overset{\text{charge}}{\rightleftharpoons}} Li_{(1-x)}MO_2 + Li_xC_6 \quad (4)$$

where M = Co or Ni.

The $LiMO_2$ compounds may be synthesized by high-temperature reactions between lithium oxide and selected transition metal oxides. For instance, $LiCoO_2$ can be prepared by heating a pelletized mixture of lithium hydroxide and cobalt carbonate in air at 850 °C [33] while $LiNiO_2$ is obtained [34] by annealing at 850 °C an intimate mixture of Li_2O and NiO. However, regardless of the type of preparation, the $LiMO_2$ compounds may easily exhibit non-stoichiometry, generally due to an excess of M. Since some M may occupy the sites available for the lithium ions, the excess stoichiometry may ultimately affect the specific capacity and the electrochemical response of the $LiMO_2$ electrodes. Therefore, the control of synthesis conditions is critical in assuring optimum performance. Practical cathode formulations involve mixtures of the $LiMO_2$ powder, carbon and binder to form a film backed on metallic (often aluminum) substrates.

Among the $LiMO_2$ compounds, $LiCoO_2$ is the one which has attracted particular attention because of its high voltage, namely around 4.5 V versus Li, a value which is consistent with the high oxidizing power of the Co^{4+}/Co^{3+} couple [33]. Complete removal of lithium ($x=1$) in eqn. (4)) from $LiCoO_2$ cannot be accomplished due to the instability of the highly reactive CoO_2 form; therefore, the cycleability of $LiCoO_2$ is generally limited to $x=0.5$, this giving a practically achieved specific capacity of 137 mAh g^{-1}. A first cycle intercalation voltage (versus Li)–composition curve for the $Li_{(1-x)}CoO_2$ electrode is illustrated in Fig. 6. As shown by Plichta *et al.* [35, 36] and

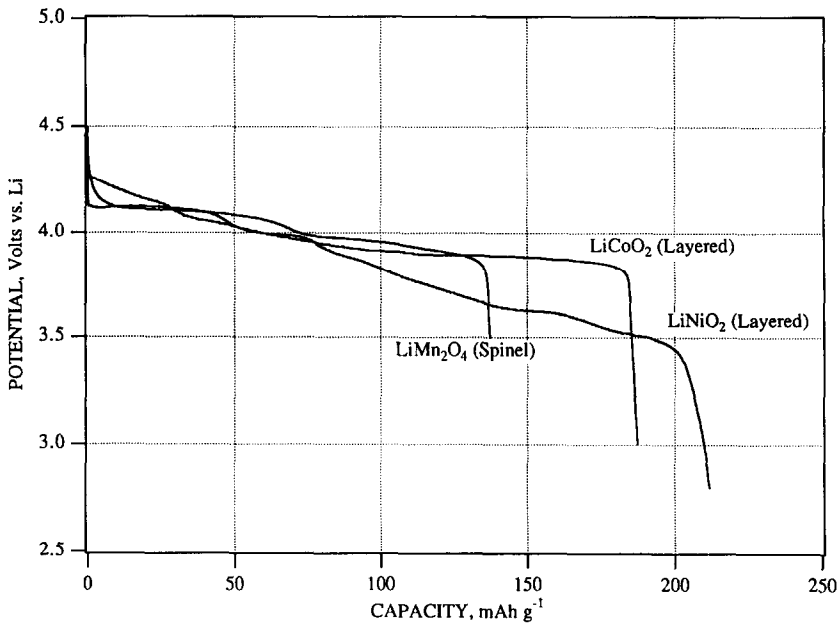

Fig. 6. Potential–capacity curves for the $LiCoO_2$, $LiNiO_2$ and $LiMn_2O_4$ cathode compounds. Electrolyte: $LiN(CF_3SO_2)_2$/EC-DEC; lithium coin half-cell; room temperature; discharge rate: 0.1 mA cm^{-2}.

recently confirmed by Reimers and Dahn [37], the deintercalation of lithium induces phase transitions which are accompanied by lattice distortion. The occurrence of the phase transitions is revealed by the plateau regions in the composition curve of Fig. 6. First cycle delivered capacities are substantially higher than in subsequent cycles.

As already mentioned, the structure of $LiCoO_2$ may be described as layered arrangements of Co and Li in a rock salt-type lattice. Removal of lithium results in interlayer expansion rather than in the most commonly expected contraction, this probably being due to increasing electrostatic replusions between O^{2-} centers upon delithiation [38]. The lattice expansion favors the extraction of the lithium ions, and thus the diffusions kinetics of the electrochemical process is expected to be fast. The diffusivity of the Li^+ ions in $Li_{(1-x)}CoO_2$ has been investigated by various authors. However, the results are contradictory. Mizushima *et al.* [33] using a transient technique, obtained a value of chemical diffusion coefficient $D=5\times10^{-9}$ cm^2 s^{-1} for x in the 0.2 to 0.8 range. A similar value was obtained by Kikkawa *et al.* [39] while Thomas *et al.* [40] reported a value of $D=5\times10^{-8}$ cm^2 s^{-1} as determined by impedance spectroscopy. Considering an average value of $D=10^{-9}$ cm^2 s^{-1} one can assume that the lithium diffusivity in $LiCoO_2$ is sufficiently fast to make this electrode quite suitable for high-rate RCBs. Indeed, the C/$LiCoO_2$ combination is the one which has been adopted by the Sony Company in its pioneering commercial product. Presently, many other companies are using this same chemistry. More detailed description of the performance and of the commercial impact of practical C/$LiCoO_2$ RCBs will be given in section 5.

The other well-known member of the $LiMO_2$ family is lithium nickel oxide, $LiNiO_2$. Nickel is an abundant material and its electrochemical use in the battery industry has been largely acquired in the production of the common nickel–cadmium cells. All these facts make $LiNiO_2$ a very attractive electrode material for the new generation rocking-chair lithium battery development. The $LiNiO_2$ compound has a structure basically consisting of octahedral sites between adjacent close-packed oxide layers, while Li^+ ions occupy the remaining sheets of octahedral sites between the oxide layers [34].

Similar to $LiCoO_2$, $LiNiO_2$ also acts as a lithium source electrode with an exchangeable amount of lithium which again averages around $x=0.5$, thus giving a practically achieved specific 'recycleable' capacity of 137 mAh g^{-1}. The variation of the voltage (versus Li) in dependence of the lithium content in the $Li_{(1-x)}NiO_2$ electrode during the first cycle is shown in Fig. 7. The Figure shows the first charge/discharge voltage profile for $LiNiO_2$ versus Li between the voltage limits of 4.5 and 2.8 V at a constant current of 0.1 mA cm^{-2} along with the derivative (dC/dV) of the voltage profile. Overall, to a charge potential of 4.5 V, 264 mAh g^{-1} or approximately 96% of the theoretical lithium capacity was removed from the $LiNiO_2$ structure. On the subsequent discharge, however, only 211 mAh g^{-1} (0.77 F/mol) of lithium could be intercalated. As can be seen in Fig. 7, there is significant character in the voltage profile, suggesting the formation of multiple phases during the intercalation-deintercalation process. Between 4.2 and 4.5 V, two additional peaks observed in the derivative plot of the charge half-cycle are absent in the discharge half-cycle, indicating that they are largely irreversible. Up to 4.15 V, the intercalation reactions appear to be highly reversible. Beyond 4.15 V, the stability of $LiNiO_2$ is questionable causing poor cycling and safety concerns [41].

The Li^+ chemical diffusion coefficient in $Li_{(1-x)}NiO_2$ has been determined by Bruce *et al.* [34] by impedance spectroscopy as $D=2\times10^{-7}$ cm^2 s^{-1}. Such a high value would suggest that $Li_{(1-x)}NiO_2$ is a very promising and convenient electrode for

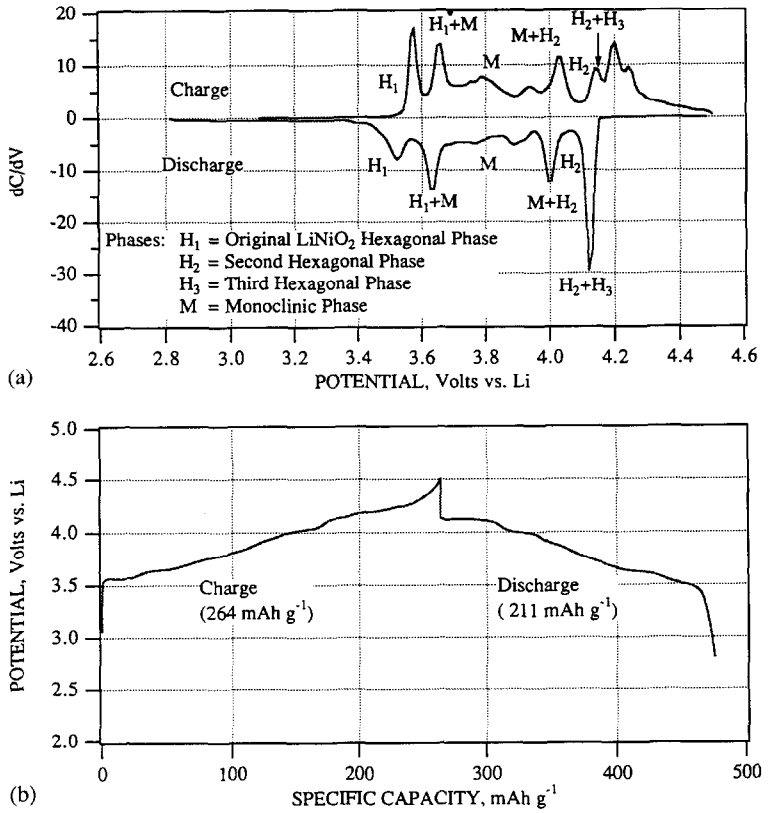

Fig. 7. (a) Voltage–capacity profile and (b) derivative plot for the first cycle charge/discharge of $LiNiO_2$ electrode (vs. Li) using 1.0 M $LiN(CF_3SO_2)_2$/EC–DEC (50:50) electrolyte solution. The phase assignments were taken from Ref. 41. Charge/discharge rate = 0.1 mA cm^{-2}.

high-rate RCBs, as indeed demonstrated by the performance of C/$LiNiO_2$ prototypes presently under development (see section 5).

The third actual choice in terms of rocking-chair cathode materials, is the spinel $LiMn_2O_4$, a high-energy, low-cost and environmental friendly compound. The general formula for spinel compounds is $A(B_2)X_4$ which has a cubic structure and can be viewed as a combination of the rock salt and zinc blend structures. The X ions are in face-centered cubic close packing, with A ions and B ions occupying the tetrahedral and octahedral sites respectively. Thackeray and Goodenough [42], reported that the $(B_2)X_4$ host framework structure can be preserved during lithiation of this compound and the Li ions are quite mobile within the interstitial site. Therefore, they proposed that a spinel compound such as $LiMn_2O_4$ can be used for applications as electrodes in rechargeable lithium cells.

The most common preparation procedure is run by reacting stoichiometric amounts of Li_2CO_3 and MnO_2 in air at 800 °C. As already stressed for the case of the $LiMO_2$ compounds, the synthesis conditions are very critical in assuring best performance for the $LiMn_2O_4$ electrode and extensive attention is presently devoted to this aspect with the final goal of defining the most efficient synthesis routes.

TABLE 1

Properties and characteristics of RCB cathode materials

Cathode	Specific capacity	Self-discharge rate	Cost	Environmental compatibility
$LiCoO_2$	Fair	Fair	Very high	Fair
$LiNiO_2$	Fair	Good	Fair	Fair
$LiMn_2O_4$	Low	Good	Very low	Excellent

The voltage (versus Li)–composition curve for the $LiMn_2O_4$ electrode is shown in Fig. 6. The removal of lithium can be extended to $x=1$ and one can easily see that the process develops over two plateaus with a practically achieved specific capacity of 120 mAh g^{-1}. However, a loss of capacity of about 20% is usually observed upon cycling the $LiMn_2O_4$ electrode. Since practical electrode configurations involve blends of $LiMn_2O_4$ powder with carbon black and a binder, the loss of capacity has been attributed to lack of interfacial contact and non-homogeneity in the electrode structure [43]. Other interpretations include spontaneous reactions and/or dissolutions in the electrolyte. Recently reported results suggest that consistent improvement in capacity retention may be obtained not only by optimizing the blending morphology but also, and particularly, by refining the synthesis procedures of the $Li_{(1+x)}Mn_2O_4$ compound, either by controlling the cooling rate [44] or by adding traces of carbon [45] or by reducing the Mn^{3+} ion concentration in the initial spinel electrode [46].

In the full composition range the $[Mn_2]O_4$ framework of an $LiMn_2O_4$ spinel possesses a three-dimensional space via face-sharing octahedra and tetrahedra and this provides conducting pathways for the insertion and the extraction of Li^+ ions. The favorable structural situation should assure a high mobility of the Li^+ ions in the manganese spinel. However, the experimentally obtained D_{Li^+} values are somewhat controversial. Dickens and Reynolds [47] have reported a value of the order of $D_{Li^+}=10^{-11}$ cm^2 s^{-1} at 25 °C for the $Li_{0.4}Mn_2O_4$ composition, which would suggest a relatively low Li^+ ion mobility, and thus a low power capability for the $C/LiMn_2O_4$ cell. In contrast, Guyomard and Tarascon [12] found a value more compatible with the structural expectation, namely a D_{Li^+} of the order of 10^{-9} cm^2 s^{-1} at room temperature, leading to the provision that $LiMn_2O_4$-based RCBs are expected to sustain high current rates.

More detailed study is certainly welcomed to define the most suitable technique for the accurate determination of reliable and reproducible diffusion coefficient data in RCB electrodes, as well as in the generality of the intercalation electrodes. In the particular case of the $LiMn_2O_4$ electrode a possible low lithium-ion diffusivity might in principle limit the cycling capability and thus penalize $LiMn_2O_4$ in respect to the $LiMO_2$ electrodes. However, as shown in Table 1, where the characteristics of three cathode materials are compared, $LiMn_2O_4$ has very favorable low cost and non-polluting advantages which ranks it in a very competitive position. The final choice of the cathode to be used in practical RCBs depends upon the specific requirements and conditions of manufacturer, and indeed all three materials, namely $LiCoO_2$, $LiNiO_2$ and $LiMn_2O_4$ are currently exploited in the RCB technology.

4. RCT (rocking chair technology) polymer electrolytes

The suitable development of RCBs requires the use of a non-aqueous electrolyte having a high conductivity (to minimize *IR* drops), a wide electrochemical stability

window (to be compatible with the high voltage cathodes), and a lithium transference number approaching unity (to reduce concentration polarization and chemical compatibility with the electrode materials. In section 2 we have shown that liquid electrolytes using proper salts (e.g., the $LiPF_6$ salt) in combination with proper solvent mixtures (e.g., the EC–DMC mixture) are presently the most common choices. However, obvious desires of improvements in reliability and design flexibility call for the replacement of the liquid solution by a solid or plastic-like electrolyte, providing that the latter maintains comparable electrochemical and electrical properties. Very promising in this respect are electrolyte membranes formed by trapping liquid solutions into polymer cages. The immobilizing procedure varies from case to case and include UV crosslinking, gelification and casting. Typical examples are membranes obtained by the gelification and casting of organic liquid solutions (e.g., solutions of a lithium salt, LiX, in a mixture of propylene carbonate (PC), and ethylene carbonate (EC) in poly(acrylonitrile) (PAN), and poly(methylmethacrylate) (PMMA) networks. These gel-type electrolyte systems, which were originally described by Feullade and Perche [48] and further characterized by Abraham and co-workers [49, 50], by Scrosati and co-workers [51–53], and by Halpert and co-workers [54] when properly prepared, are dimensionally stable and highly conducting, and thus they offer a very favorable and unique combination of mechanical-electrochemical properties. For instance, the membrane formed by tapping into a poly(acrylonitrile) matrix a solution of lithium perchlorate in a propylene carbonate/ethylene carbonate mixture, here briefly indicated as PAN–PC/EC–$LiClO_4$, has a room temperature conductivity of 4.5×10^{-3} S cm^{-1} (see Table 2), i.e., a value comparable with that of the parent $LiClO_4$–PC liquid solution (3.0×10^{-3} S cm^{-1}).

Figure 8 illustrates the Arrhenius plots of typical examples of PAN-based and PMMA-based membranes, while Table 2 lists the electrochemical properties of a variety of systems differing from the lithium salt–solvent combination. The reported data show that the conductivity averages around 10^{-3} S cm^{-1} at 25 °C and remains exceptionally high even at temperatures well below ambient. Such as an outstanding transport performance is certainly the feature which places these membranes among the most appealing new generation gel-type polymer electrolytes. Furthermore, the fast ionic

TABLE 2

Electrochemical properties at 25 °C of gel-type PAN-based and PMMA-based electrolytic membranes

Electrolyte	Conductivity (10^{-3} S cm^{-1})	Lithium transfer number	Anodic stability (V)
PAN–PC/EC–$LiClO_4$	4.5	0.5–0.6	4.8
PAN–PC/EC–$LiAsF_6$	4.6	0.6–0.7	4.5
PAN–PC/EC–$LiN(CF_3SO_2)_2$	2.0	0.7–0.8	4.6
PAN–BL–$LiClO_4$	4.4	0.5–0.6	4.9
PAN–BL–$LiAsF_6$	6.0	0.6–0.7	4.6
PAN–BL–$LiN(CF_3SO_2)_2$	4.0	0.7–0.8	4.7
PMMA–PC–EC–$LiAsF_6$	0.8	0.6	4.8
PMMA–PC–EC–$LiN(CF_3SO_2)_2$	0.7		4.9

PC = propylene carbonate; EC = ethylene carbonate; BL = γ-butyrolactone; PAN = poly(acrylonitrile), and PMMA = poly(methylmethacrylate).

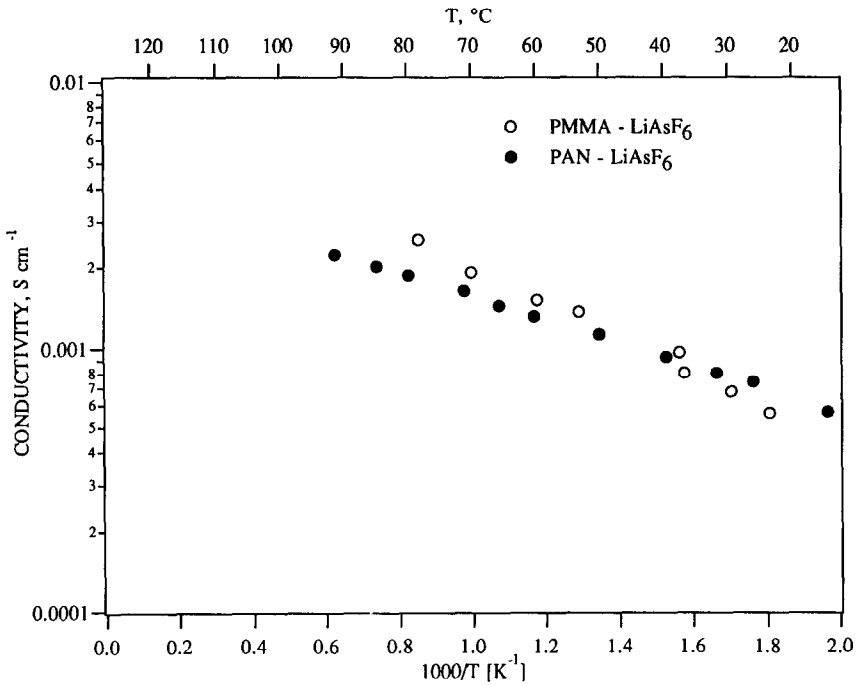

Fig. 8. Arrhenius plots of PAN–PC/EC–$LiAsF_6$ and of PMMA–PC/EC–$LiAsF_6$ membranes having the following molar compositions: 16-23-55.6-4.5 and 30-19/46.5-4.5.

transport is combined with other key features, such as wide electrochemical stability and high lithium transference number [52] as again illustrated in Table 2.

Some important general considerations may be outlined for these ionically conducting membranes, namely:

(i) Their electrochemical stability exceeds, on average, 4.5 V versus Li and this demonstrates that they are compatible with the high-voltage RCB electrodic couples.

(ii) Their lithium transference number is, on average, higher than that usually obtained for the parent pure liquid solutions. This suggests that the role of the polymer component (PAN or PMMA in the case of this work) is much more complex than that of acting as a porous solid support for the liquid solution.

The high electrochemical stability and the unusually high lithium transference number make these membranes almost ideal electrolytes for new type, advanced design, RCBs, where the characteristics of safety and cycleability, uniquely associated to the electrode nature, are combined with those of plasticity and conductivity, uniquely associated to the nature of the electrolyte. Indeed, many academic and industrial laboratories are presently attempting to verify this fascinating concept [46, 31] and the feasibility of the fabrication of laminated, thin-layer RCBs has been already announced [55, 56].

5. Practical RCBs

Sony Energytech Incorporated announced the introduction of 'lithium-ion rechargeable batteries' on February 1990, using the $C/LiCoO_2$ couple in cylindrical cell

configurations [8]. Since then, many announcements were made with improvements to the system's energy density and rate capability. Table 3 shows a comparison of lithium-ion technologies being developed by various companies. The list is not inclusive of all companies in the field but rather, summarizes those who have published information on this technology. RCB cells are now being made in small button cell configurations to large cylindrical or prismatic sizes. More recently, flexible plastic electrolyte batteries were announced with performance characteristics (e.g., cycle life and rate capability) almost equal to those with liquid electrolyte [56]. Future improvements will concentrate on improving electrode's specific energy, processability and making cell cost competitive with other aqueous systems (e.g., nickel–cadmium and nickel–metal hydride).

Table 4 shows the performance of the most prominent RCB sizes from Sony Corporation. The first two digits of 14 500 stands for the diameter in mm and the next two digits for the height in mm. The 14 500- and 20 500-types were introduced in cellular phones, the 18 650 in 8 mm video-type recorders, and 16 630 in mini-disc drives. Recently a new laptop was introduced with nine 186 500 cells in series-parallel connections. To date this is the largest battery pack directed towards a consumer application [57].

The following characteristics summarize the behavior of practical RCBs for consumer and other industrial applications.

Intrinsic safety

No safety problems were reported on commercial RCBs since their introduction more than three years ago for two main reasons. The first is the many electronic safety features incorporated in the battery pack (e.g., voltage–current regulations, switches, and fuses, etc.) that assured safe handling. This is beyond the scope of this review. The second is the inherent safety behavior of RCBs due to no dendritic growth, absence of stack pressure and minimum thermal runaway after abusive treatment. Von Sacken *et al.* [58] used an accelerating rate calorimeter (ARC, Columbia Scientific Instruments) to probe the thermal stability of the coke electrode as a function of specific surface area, lithium content and choice of electrolyte. They used the AA-size as a test vehicle with manganese oxide cathode and metallic lithium versus petroleum coke anode. Low surface area carbon, say less than 10 $m^2\ g^{-1}$, anode-limited design of RCB cells and the selection of EC-based electrolyte, all resulted in less heat build-up in the ARC instrument as compared with metallic lithium cells, thus, improved safety. There is a wide belief now that the morphology of the dendritic metallic lithium growth cannot be controlled which makes the ultimate safety of cycled cells difficult to predict. Only recently this belief is being challenged [59].

High energy density, power density and cumulative energy

High energy density is an attractive feature of RCBs. Values above 100 Wh kg^{-1} and 300 Wh l^{-1} have been reported [8, 13]. The penalty of a carbon with 372 mAh g^{-1} has not adversely affected cell capacity nor energy density. Because of the excess metallic lithium and its low packing density, the practical energy density from carbon equals or exceeds that of metallic lithium (Table 5). Experimental AA-cells with the carbon anode have demonstrated higher power density (e.g., higher voltage and drain rate) and higher cumulative energy density (e.g., longer cycle life) than metallic lithium anode cells. For these reasons, RCBs have attracted much attention as competitive systems to rechargeable aqueous systems (e.g., alkalines, lead/acid, Ni–Cd, Ni–MH).

Table 6 shows the performance–cost relationship of various battery chemistries for various applications. Our estimates show the RCB system to be competitive

TABLE 3

Comparison of lithium-ion technologies being developed by various companies[a]

Manufacturer	Anode material	Cathode material	Nominal operational voltage (V)	Cell types	Cell sizes	Status
Sony	Petroleum, coke	$LiCoO_2$	3.6	Cylindrical	14500, 20500, 18650, 16630, 26XXX	Full production
				Square	48 mm×40 mm×8 mm 48 mm×34 mm×8 mm	
Panasonic	Graphite	$LiCoO_2$	3.6	Cylindrical	17500, 18650	Sampling
				Square	40488	
Sanyo	Graphite	$LiCoO_2$	3.8	Cylindrical	18650	Sampling
Toshiba	LGH	V_2O_5	3.0	Coin	2025, 2430	Full production
		$LiCoO_2$	3.6			
				Cylindrical	18506, 18650, 18835	Full production
VARTA	Graphite	$LiCoO_2$	3.6	Unknown	Unknown	Pilot line
Rayovac	Petroleum, coke	$LiNiO_2$	3.3	Coin	1225, 2335	Pilot line
				Cylindrical	AA, D	Experimental
Bellcore	Petroleum, coke	$LiMn_2O_4$	3.6	Experimental cells only	4.2 cm×7.6 cm×0.6 cm	Experimental
SAFT	Petroleum, coke	$LiNiO_2$	3.3	Cylindrical	D	Pilot line

[a]Above information obtained from open literature and personal communications.

TABLE 4

Performance of Sony lithium-ion batteries

Cell type	14500	16630	20500	18650
Physical				
Volume (cm^3)	7.5	12.0	16.5	17.06
Weight (g)	18.0	29.0	39.0	49.0
Electrical				
Voltage (V)	3.6	3.6	3.6	3.6
Capacity (mAh)	450	750	1200	1200
Energy (Wh)	1.62	2.7	4.32	4.32
Energy density				
Per volume (W h l^{-1})	216	225	261	253
Per weight (Wh kg^{-1})	90	93	110	108
Cycle life (cycles)	1200	1200	1200	1200
Temperature effects				
Self-discharge after 1 month at 23 °C (%)	8	8	8	8
Charge temperature (°C)	0/45	0/45	0/45	0/45
Discharge temperature (°C)	−20/+60	−20/+60	−20/+60	−20/+60

(¢ per Wh) with lead/acid and Ni–Cd. At the present time, however, RCBs are highly prized.

Long cycle life

Evaluation of the 20 500 cylindrical cell from Sony ($C/LiCoO_2$) after 1200 cycles was investigated by nuclear magnetic resonance, impedance spectroscopy and microscopic examination [60]. The cells retained 77% of their initial capacity after 1200 cycles (100% depth-of-discharge) with no swelling or separation of the electrodes from the current collector. The studies revealed the majority of lithium in both electrodes is in an ionic form, not metallic even after 1200 cycles. The impedance of the cathode did not drastically change between initial and 1200 cycles, but the impedance of the anode increased from 61.5 to 269.0 mΩ (4.4 fold increase). This increase in carbon impedance was postulated to be the result of a solid electrolyte interface (SEI) growth which came about by electrolyte decomposition.

Microscopic examination of the anode surface revealed the presence of small amounts of 'inactive' lithium deposits. The shape of lithium deposits were affected by the salt used in PC–DEC mixed solvent. 'Spherical' lithium deposits were formed in the electrolyte using $LiPF_6$ as a salt while 'dendritic' lithium deposits were formed when $LiClO_4$ was used. Indeed, the $LiPF_6$ salt has been selected as the salt of choice for many commercial RCBs since the 'spherical' lithium deposits are inherently safer than 'dendritic' lithium deposits.

Further microscopic examination of the cathode and anode surfaces and electrode total thickness revealed no swelling, deterioration or dimensional changes after 1200 cycles. This is an important finding in these types of batteries since Li^+ insertion during intercalation and deintercalation will have a tendency to 'wear out' or collapse some of the lattice structure of the layered cathode or crystallites-organized portions of the carbon anode. Indeed, we have found that cathode integrity plays an important role in electrode cycleability. Figure 9 shows the cycle-life performance of coin cells

TABLE 5

Capacity, rate capability and cumulative energy

Characteristics	Carbon	Metallic lithium	Ratio (C/Li)
Capacity			
Theoretical density (g cm^{-3})	2.25 (graphitic carbon)	0.53	
Practical density with conductive diluent	1.60	0.53	
Theoretical capacity (mAh g^{-1})	372	3862	
Practical capacity (mAh g^{-1})	316 (85% active material)	772 (5-fold excess Li)	
Theoretical capacity (mAh cm^{-3})	837	2047	
Practical capacity (mAh cm^{-3})	506	409	
Practical capacity ratio			1.24
Rate capability (AA-size)[a]			
Average cell voltage (V)	3.6	2.6	
Average drain at 1 h (mA)	300	100	
Average drain ratio			3.00
Cumulative energy (AA-size)[a]			
Cell capacity (mAh)	600	600	
Energy per cycle (Wh)	2.16	1.56	
Cycle life	1200	200	
Cumulative energy (kWh)	2.59	0.312	
Cumulative energy ratio			8.30

[a]Values based on non-optimized experimental cells.

with calendered electrodes (polytetrafluoroethylene (PTFE) binder) versus those with pressed pellets using an ethylene/propylene/diene monomer (EPDM) binder. No failure was observed at 1200 cycles with the PTFE binder while the EPDM binder had a capacity fade. It is interesting to note that the electrode thickness in the coin cell is about 1.0 mm versus 0.25 mm or less in cylindrical cells [61].

An obvious way to boost cell capacity is to raise the charge voltage from 3.7 to 4.0 V (C/$LiNiO_2$). Up to 40% increase in capacity at a higher operating voltage was realized at 4.0 V (Fig. 10). Raising the voltage will enhance Li^+ intercalation. As discussed earlier, however, care must be exercised not to exceed certain upper limit values (e.g., 4.15 V for $LiNiO_2$, 4.2 V for $LiCoO_2$ and 4.5 V for $LiMn_2O_4$) because of collapsing of the layered structure and/or electrolyte decomposition. These factors may result in premature failure (e.g., increased capacity fade, gas generation, etc.) and will compromise the safety features of these batteries.

At 30% depth-of-discharge, the cycle life from coin cells can be extended. Figure 11 shows up to 3000 cycles from the 1225 coin cell at 2.0 mA cm^{-2} without failure.

Improved rate capability

By rate capability, we mean the ability to fast charge/discharge RCBs at the 1*C* rate or better. The failure of Ni–Cd acceptance by consumers had been traced to the

TABLE 6

Performance–cost/applications, AA-size

Characteristic	Battery system						
	Primary alkaline	Lead/acid	Secondary alkaline	Nickel–cadmium	Nickel–metal hydride	Lithium–manganese	RCB
Estimated value							
Performance							
Capacity (Ah/cell)	2.2	0.3	0.75	0.70	1.0	0.6	0.5
Working voltage (V)	1.25	2.0	1.25	1.20	1.20	2.5	3.0
Wh/cycle	2.75	0.6	0.94	0.84	1.20	1.50	1.50
No. of cycles	1	400	30	400	500	200	800
Wh/all cycles	2.75	240	28	336	600	300	1200
Retail price ($/cell)[a]	0.75	1.00[b]	1.40	2.50	5.00	7.00	5.00
Value							
¢/Wh	27.27	0.41	5.00	0.74	0.83	2.33	0.42
Ratio vs. alkaline	1	0.015	0.183	0.027	0.030	0.085	0.015
Consumer/industrial applications							
Photoflash	Yes	Yes	Yes	Yes	Yes	Yes	Yes
Radio	Yes	No	Yes	Yes	Yes	No[c]	Yes
Cassette	Yes	No	Yes	Yes	Yes	No	Yes
Toys	Yes	No	Yes	Yes	Yes	No	Yes
Tools	No	Yes	No	Yes	No	No	(Yes)
Camcorders	Yes	Yes	Yes	Yes	Yes	No	Yes
Meters/instruments	Yes	Yes	Yes	Yes	Yes	Yes	Yes
SLI, EV, UPS, etc.	No	Yes	No	(Yes)	(Yes)	No	Yes
OEM/government applications							
Laptop	No	Yes	No	Yes	Yes	Yes	Yes
Cordless phones	No	Yes	No	Yes	Yes	No	Yes
Medical	No	Yes	No	No	Yes	No	Yes
Government	No	Yes	No	No	Yes	Yes	Yes

[a]Based on full scale production. [b]Estimated (cells size not commercially available). [c]Safety problems.

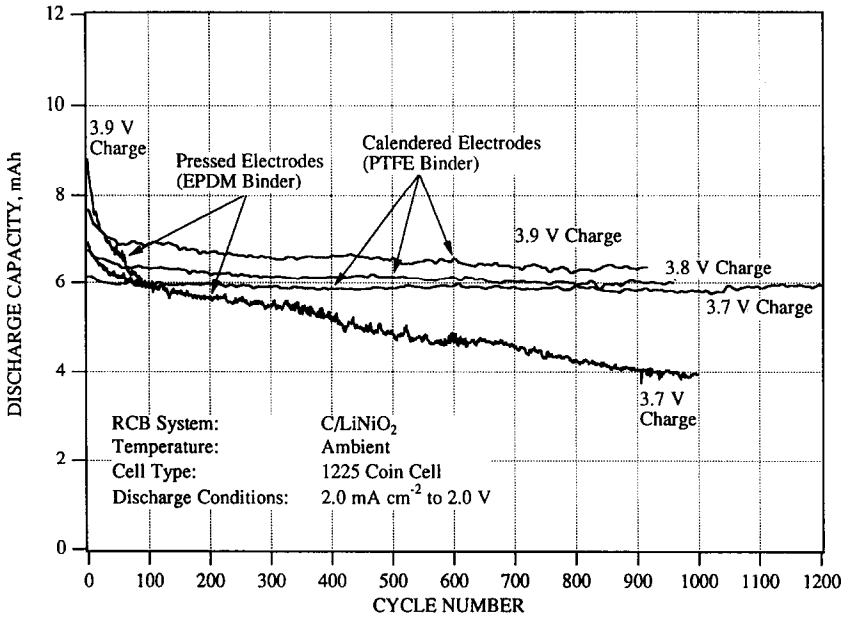

Fig. 9. The effect of binders on the cycle life of 1225 RCT coin cells (diameter: 12 mm, diameter height: 2.5 mm).

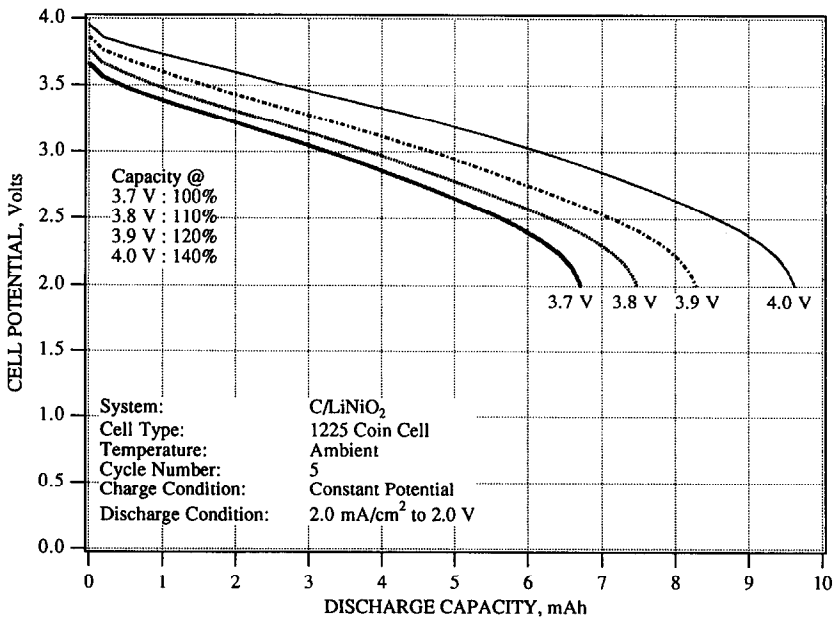

Fig. 10. Charge voltage vs. cell capacity and operating voltage.

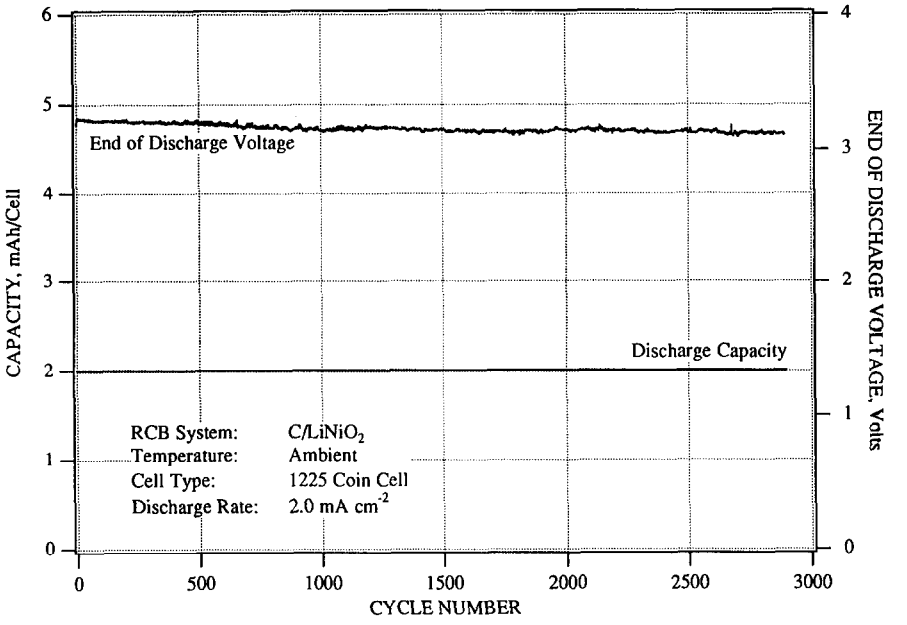

Fig. 11. Cycle numbers from RCT-1225 coin cells at 30% depth-of-discharge.

long charge time (overnight) which created an inconvenience. Even in a multicell battery pack, a low cost and fast charger will be a welcome relief.

Fast charging of Ni–Cd batteries has been accomplished via high rate electrode design (e.g., foam or fiber) and appropriate chargers. With RCB design, rate capability is influenced by carbon selection, electrode integrity (e.g., thickness, adhesion to current collectors) and electrolyte conductivity. We have used an equation developed by Selim and Bro [62] to predict the discharge/charge rates of RCB electrodes as follows:

$$Q = \frac{Q_0^* \tanh\left(\frac{i}{R}\right)^{1/A}}{\left(\frac{i}{R}\right)^{1/A}} \tag{5}$$

where:
i = cell current density, mA cm^{-2};
Q = delivered capacity at current density (i), mAh;
Q_0 = empirical parameter representing the standard capacity of the cell which is the maximum capacity that can be realized from the cell at infinitely low rates of discharge, mAh;
R = empirical parameter representing the standard rate of the cell beyond which the delivered capacity will begin to decline rapidly, mA cm^2, and
A = empirical parameter representing the accommodation coefficient of the cell which is inversely proportional to the rate of decline in capacity at rates above the standard rate. Therefore, the higher the value of A, the better the rate capabilities of the cell.

Cells (C/LiNiO$_2$) are usually cycled at a given charge or discharge rate, then allowed to rest before receiving decreasing rates. The discharge capacity is plotted

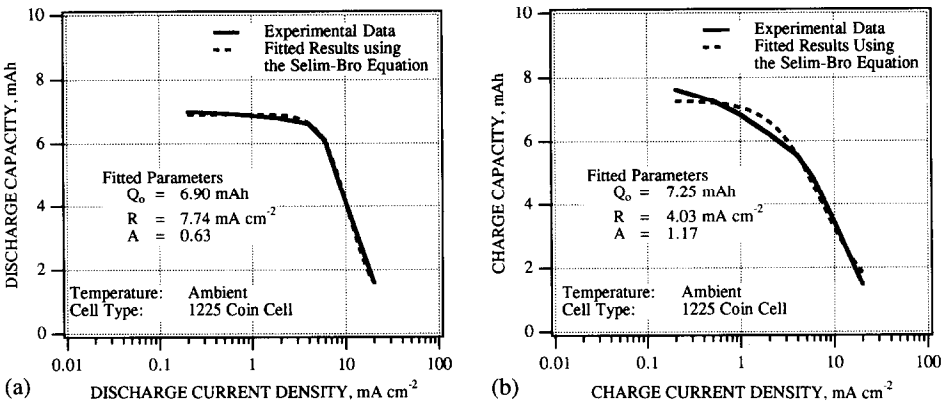

Fig. 12. Rate capability evaluation using the Selim–Bro equation from Ref. 61: (a) discharge-rate evaluations, and (b) charge-rate evaluations.

versus current density and the values are fitted using eqn. (5). Data in Fig. 12 show maximum charge rate of 4.03 mA cm^{-2} and maximum discharge rate of 7.74 mA cm^{-2} for 1.0 mm thick electrodes. Thinning the electrodes by a factor of four should improve the rate capability to more than double. For an in-house built D-cell size with 1200 cm^2 of surface are and a capacity of 4000 mAh, a charge rate of 0.8 h and a discharge rate of 1.5 h is possible with 90% efficiency. In a similar work by Sony (C/$LiCoO_2$) on D-cell size with 3900 mAh, the 1.0 and 0.5 h discharge rates were reported at 93% and 82% efficiency. Further improvements are expected by thinning the electrodes, the use of graphite microfibers (whiskers) and more conductive electrolyte–binder system. Cycling RCBs at high drain rates (10 to 15 min) will be a challenge for future work.

Temperature effects

At ambient storage or discharge, RCBs have higher capacity loss than metallic lithium batteries but lower than aqueous rechargeables (e.g., lead/acid, Ni–Cd and Ni–MH). Similar results were reported at elevated temperatures [18, 59]. With metallic lithium Broussely *et al.* [63] showed Li_xNiO_2 to be more stable than Li_xCoO_2 after one month storage at 45 °C. Our results support this finding even with carbon anodes. $LiNiO_2$ is compatible with more types of electrolyte solutions than $LiCoO_2$ because of lower charge voltage and more stable electrode kinetics. Whether capacity loss in RCBs at elevated temperatures is due to a cathode or an anode phenomenon has to be determined. The electrolyte solution, however, will play an important role in this decision. Ozawa and Yokokawa [60] reported an 8% capacity loss after one month of ambient temperature storage. This capacity loss is mostly recoverable. At elevated temperatures further solvent interaction with the intercalated carbon will result in higher irreversible capacity with extended storage. Better values need to be developed with an explanation of each failure mode. This is being done in one of our laboratories.

6. Summary

RCBs represent a unique opportunity to the battery industry to reach a step closer toward the ideal battery. The recent Bellcore announcement of a flexible plastic battery using low-cost spinel cathode is an encouraging step in the right direction.

Engineering carbons with capacity higher than LiC_6 (372 mAh g^{-1}) and the discovery of an innovative cathode material with higher capacity than $Li_{(1+x)}Mn_2O_4$ (120 mAh g^{-1}) should result in better RCBs. Even with the present technology as reported in this review, RCBs are very attractive as compared with existing rechargeable aqueous systems.

Remaining to be resolved are the scale-up production issues to make the battery affordable to the consumer. These issues are beyond the scope of this review but nevertheless, represent a challenging task for battery engineers worldwide.

Acknowledgements

This work has been supported by the Consiglio Nazionale delle Ricerche, Progetto Strategico Batterie Leggere and the Rayovac Corporation.

References

1 M.S. Whittingham, *Prog. Solid State Chem., 12* (1978) 1.
2 D.W. Murphy and P. Christian, *Science, 205* (1979) 651.
3 C.A. Vincent, F. Bonino, M. Lazzari and B. Scrosati, *Modern Batteries,* E. Arnold, London, 1984.
4 K. Shahi, J.B. Wagner and B.B. Owens, in J.P. Gabano (ed.), *Lithium Batteries,* Academic Press, London, 1983, p. 407.
5 C.A. Vincent, *Prog. Solid State Chem., 17* (1987) 145.
6 K.M. Abraham, in B. Scrosati (ed.), *Applications of Electroactive Polymers,* Chapman and Hall, London, 1993, p. 75.
7 M. Armand, in D.W. Murphy, J. Broadhead and B.C.H. Steele (eds.), *Materials for Advanced Batteries,* Plenum, New York, 1980, p. 145.
8 T. Nagaura and K. Tozawa, *Prog. Batteries Solar Cells, 9* (1990) 209.
9 T. Ohzuku, A. Ueda and M. Nagayama, *J. Electrochem. Soc., 140* (1993) 1862.
10 K. Brandt, *Proc. 7th Int. Meet. Batteries, Boston, MA, USA, May 15–20, 1994,* Abstr. FRI-03.
11 R. Yazami and G. Guerard, *J. Power Sources, 43* (1993) 39.
12 D. Guyomard and J.M. Tarascon, *J. Electrochem. Soc., 139* (1992) 937.
13 S.A. Megahed and W.B. Ebner, *Proc. 9th Annual Battery Conf. Applications and Advances, Long Beach, CA, USA, 1994.*
14 M.J. Rosolen, S. Passerini and B. Scrosati, *J. Power Sources, 45* 1993) 333.
15 J.R. Dahn, *Phys. Rev. B: Condens. Matter, 44* (1991) 9170.
16 J.R. Dahn, A.K. Sleigh, H. Shi, B.M. Way, W.J. Wegdanz, J.N. Reimers, Q. Gong and U. von Sacken, in G. Pistoia (ed.), *Lithium Batteries,* Elsevier Science, Amsterdam, 1994.
17 E. Peled, *J. Electrochem. Soc., 126* (1981) 2047.
18 B. Scrosati and S. Megahed, *Proc. Fall Meet. Electrochemical Society, Short Course, New Orleans, LA, USA, Oct. 10, 1993.*
19 W. Ebner, D. Fouchard and L. Xie, *Solid State Ionics* (1994) submitted for publication.
20 W. Ebner, D. Fouchard, L. Xie and S. Megahed, *Power Sources Symp., Cherry Hill, NJ, USA, 1994,* submitted for publication.
21 W. Ruland, *Acta Crystallogr., 18* (1985) 992.
22 C.K. Huang, S. Surmpudi, A. Attia and G. Halpert, *Proc. IEEE 35th Int. Power Sources Symp.,* IEEE Customer Service Department, Piscataway, NJ, USA, 1992, p. 197.
23 R. Bitthin, R. Herr and D. Hoge, *J. Power Sources, 44* (1993) 409.
24 E. Peled, in J.P. Gabano (ed.), *Lithium Batteries,* Academic Press, London, 1983, p. 43.
25 F. Croce and B. Scrosati, *J. Power Sources, 43* (1993) 9.
26 K. Tanaka, M. Itabashi, M. Aoki, S. Hiraka, M. Katoka, S. Fujita, K. Sekai and K. Ozawa, *Fall Meet. Electrochemical Society, New Orleans, LA, USA, Oct. 1993,* Abstr. No. 21.

27 B.M. Way and J.R. Dahn, *J. Electrochem. Soc., 141* (1994) 907.
28 U. Sato, M. Noguchi, A. Deuiachi, N. Oki and M. Endo, *Science,* (Apr. 22) (1994) 556.
29 A. Vaccaro, T. Pananisamy, R.L. Kerr and J.T. Maloy, *Solid State Ionics, 6* (1981) 363.
30 H. Gerischer, F. Decker and B. Scrosati, *J. Electrochem. Soc.,* in press.
31 S. Passerini, F. Croce and B. Scrosati, *J. Electrochem. Soc.,* in press.
32 T. Ohzuku, in G. Pistoia (ed.), *Lithium Batteries,* Elsevier, London, 1994.
33 M. Mizushima, P.C. Jones, P.J. Wiseman and J.B. Goodenough, *Solid State Ionics, 3/4* (1981) 171.
34 P.G. Bruce, A. Lisokowa-Oleksiak, M.Y. Saidi and C.A. Vincent, *Solid State Ionics, 57* (1992) 353.
35 E. Plitcha, S. Slane, M. Uchiyama, M. Salomon, D. Chua and W.H. Lin, *J. Power Sources, 21* (1987) 25.
36 E. Plicha, M. Salomon, S. Slane, M. Uchiyama, D. Chua, W.B. Ebner and W.H. Lin, *J. Electrochem. Soc., 136* (1989) 1865.
37 J.N. Reimers and J.R. Dahn, *J. Electrochem. Soc., 139* (1992) 2091.
38 J. Desilvestro and O. Haas, *J. Electrochem. Soc., 137* (1990) 5C.
39 S. Kikkawaa, S. Miyazaki and M. Koizumi, *J. Power Sources, 14* (1985) 231.
40 M.G.S.R. Thomas, P.G. Bruce and J. Goodenough, *Solid State Ionics, 18/19* (1986) 794.
41 W. Li, J.N. Reimers and J.R. Dahn, *Solid State Ionics,* submitted for publication.
42 M.M. Thackeray and J.B. Goodenough, *US. Patent No. 4 507 371* (1985).
43 J.M. Tarascon, E. Wang, F.K. Shokoohi, W.R. MacKinnon and S. Calson, *J. Electrochem. Soc., 139* (1992) 2859.
44 J.M. Tarascon, W.R. MacKinnon, R. Coowar, G. Amatucci, F.K. Shokoohi and D. Guyomard, *Ext. Abstr., 7th Int. Meet. Lithium Batteries, Boston, MA, USA, May 15–20, 1994,* Abstr. No. TUE-05.
45 P.G. Bruce and H. Huang, *Ext. Abstr., 7th Int. Meet. Lithium Batteries, Boston, MA, USA, May 15–20, 1994,* Abstr. No. TUE-05.
46 R.J. Gummow, A. de Kock, D.C. Liles and M.M. Thackeray, *Ext. Abstr., 7th Int. Meet. Lithium Batteries, Boston, MA, USA, May 15–20, 1994,* Abstr. No. II-B-31.
47 P.G. Dickens and G.F. Reynolds, *Solid State Ionics, 5* (1981) 53.
48 G. Feullade and P.H. Perche, *J. Appl. Electrochem., 5* (1975) 63.
49 K.M. Abraham and M. Alamgir, *J. Power Sources, 44* (1993) 195.
50 K.M. Abraham, in B. Scrosati (ed.), *Application of Electroactive Polymers,* Chapman and Hall, London, 1993, p. 75.
51 G. Dautzenberg, F. Croce, S. Passerini and B. Scrosati, *Chem. Mater., 6* (1994) 538.
52 G.B. Appetecchi, F. Croce, G. Dautzenberg, S. Passerini and B. Scrosati, *Electrochim. Acta,* in press.
53 G.B. Appetecchi, F. Croce and B. Scrosati, *J. Electroanal. Chem.,* submitted for publication.
54 G. Nagasubramanian, A.I. Attia and G. Halpert, *J. Appl. Electrochem., 24* (1994) 298.
55 M. Alamgir and K.M. Abraham, *Ext. Abstr., 7th Int. Meet. Lithium Batteries, Boston, MA, USA, May 15–20, 1994,* Abstr. No. TUE-03.
56 A.S. Gozd, C.N. Schmutz and J.M. Tarascon, *US Patent No. 5 3296 318* (Mar. 22, 1994).
57 K. Ozawa and T. Aita, *11th Int. Seminar Primary and Secondary Battery Technology and Applications, Deerfield Beach, FL, USA, Feb 28–Mar. 3, 1994.*
58 U. von Sacken, E. Nodwell and A. Sundher, *Ext. Abstr., 7th Int. Meet. Lithium Batteries, Boston, MA, USA, May 15–20, 1994,* Abstr. No. Mon-03.
59 P. Dan, *Ext. Abstr., 7th Int. Meet. Lithium Batteries, Boston, MA, USA, May 15–20, 1994,* Abstr. No. FRI-01.
60 K. Ozawa and M. Yokokawa, *10th Int. Seminar Primary and Secondary Battery Technology and Applications, Deerfield Beach, FL, USA, Mar. 1–4, 1993.*
61 S. Megahed and W.B. Ebner, *Ext. Abstr., 7th Int. Meet. Lithium Batteries, Boston, MA, USA, May 15–20, 1994,* Abstr. No. FRI-04.
62 R. Selim and P. Bro, *J. Electrochem. Soc., 118* (1971) 829.
63 M. Broussely, F. Perton and I. Labat, *Ext. Abstr., 6th Int. Meet. Lithium Batteries, Münster, Germany, May 10–15, 1992,* Abstr. No. 92.